First publ. in: Biochemica 2 (1998), pp. 25-28

Differentiation Between Apoptotic and Necrotic Cell Death by Means of the BM Cell Death Detection ELISA or Annexin V Staining

MARCEL LEIST, SIMONE KÜHNLE, BARBARA SINGLE, and PIERLUIGI NICOTERA
Molecular Toxicology, University of Konstanz, PO-Box 5560, D-78457 Konstanz
e-mail: marcel.leist@uni-konstanz.de

Key Words
apoptosis, cell death detection, annexin staining

Abstract
Apoptosis and necrosis are two forms of cell death that have been defined on the basis of distinguishable morphological criteria. However, these different types of cell death may involve several common signalling and execution mechanisms. Since various stimuli induce both apoptotic and necrotic death, the mode of cell demise seems to be dependent on intracellular factors. One of these factors is the concentration of ATP. By modulating ATP levels, apoptosis or necrosis can be triggered selectively under otherwise identical conditions. By controlling ATP levels in staurosporine treated Jurkat cells, apoptotic (but not necrotic) cell death was detected selectively, and was quantitated with high sensitivity by the BM Cell Death Detection ELISA or by staining with annexin V.

Introduction

Initially apoptosis was defined on the basis of morphological criteria as a separate mode of cell death, clearly distinct from necrosis [1]. However, both forms of cell death can occur simultaneously or in a clearly defined temporal or spatial relation within an organ (e.g. in experimental liver failure or cerebrovascular disease/stroke). Moreover, recent evidence suggests that identical receptors, signal transduction pathways and mechanisms of cytotoxicity can be involved in apoptotic or necrotic cell death. It seems that apoptosis and necrosis represent two extremes of a broad spectrum of cell death modes. Cytotoxic pathways and morphological characteristics may be determined by different intracellular factors and external conditions [2, 3].

In multicellular organisms, the mode of cell death has considerable significance extending beyond the fate of the individual cell. Apoptotic cells are efficiently and rapidly phagocytosed before they lyse and cause inflammation. This facilitates tissue reorganisation or reconstitution in development and after damage. Moreover, processes characteristic of apoptosis prevent the spread or release of DNA from transformed or virus-infected cells. One of these processes is the selective fragmentation and packaging of cellular DNA. The genome is usually cleaved into fragments of about 300 and 50 kbp (so-called high molecular weight (HMW)-fragments). Often this is followed by oligonucleosomal DNA-fragmentation, i.e. formation of fragments of about n x 180 bp size. Although DNA-fragmentation is not causally involved in cell death, it seems to be an important feature of apoptosis in relation to the surrounding tissue, and it is often used as a diagnostic criterion.

Methods

Jurkat cells (T-cell lymphoma) were grown in RPMI 1640 medium supplemented with 10% fetal calf serum. Before the experiments, cells were washed and resuspended in serum-free medium without glucose, supplemented with 2 mM pyruvate (mitochondrial ATP-generation only). For ATP-depletion, cells were exposed to 2.5 µM oligomycin. To allow cytosolic ATP-generation only, cells were incubated in medium containing 2.5 µM oligomycin plus 5 mM glucose. Fortyfive min after addition of oligomycin, cells were incubated with the cell death inducing agent staurosporine (STS, 1.25 µM) or an agonist monoclonal antibody against CD95/Fas/Apo-1 (αCD95, 100 ng/ml). Cell death was characterized by morphological criteria, by measurement of intracellular proteolysis, and by analyzing DNA fragmentation by means of conventional agarose gel electrophoresis (CAGE) or field inverted gel electrophoresis (FIGE) as described [4]. The Boehringer Mannheim Cell Death Detection ELISA was used according to the supplier's instructions and as previously described [5]. ATP was determined luminometrically using a reagent kit (Boehringer Mannheim). Phosphatidylserine (PS) translocation was analyzed by staining with FITC-labeled annexin V (Boehringer Mannheim), by FACS analysis and by confocal microscopy as described [4, 6].

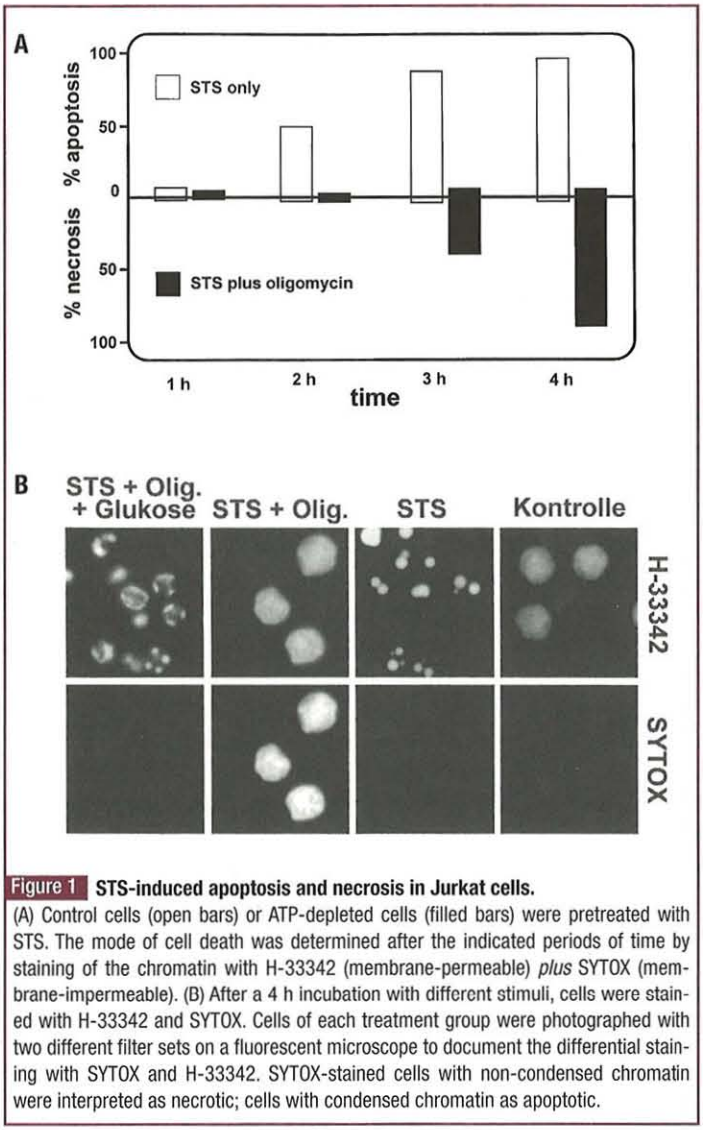

Figure 1 **STS-induced apoptosis and necrosis in Jurkat cells.**
(A) Control cells (open bars) or ATP-depleted cells (filled bars) were pretreated with STS. The mode of cell death was determined after the indicated periods of time by staining of the chromatin with H-33342 (membrane-permeable) *plus* SYTOX (membrane-impermeable). (B) After a 4 h incubation with different stimuli, cells were stained with H-33342 and SYTOX. Cells of each treatment group were photographed with two different filter sets on a fluorescent microscope to document the differential staining with SYTOX and H-33342. SYTOX-stained cells with non-condensed chromatin were interpreted as necrotic; cells with condensed chromatin as apoptotic.

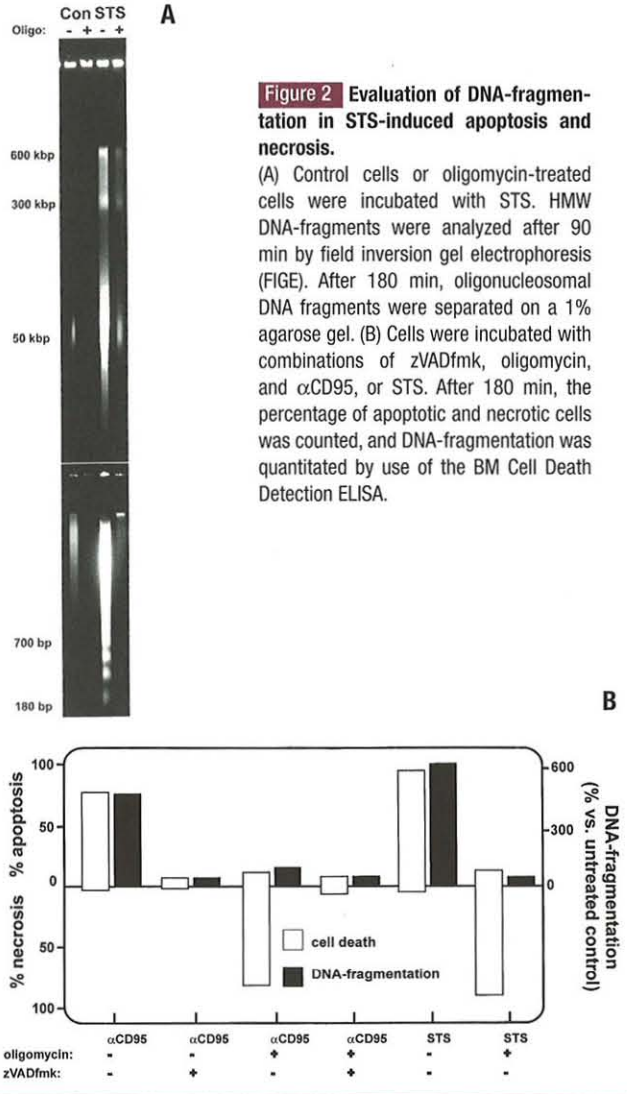

Figure 2 **Evaluation of DNA-fragmentation in STS-induced apoptosis and necrosis.**
(A) Control cells or oligomycin-treated cells were incubated with STS. HMW DNA-fragments were analyzed after 90 min by field inversion gel electrophoresis (FIGE). After 180 min, oligonucleosomal DNA fragments were separated on a 1% agarose gel. (B) Cells were incubated with combinations of zVADfmk, oligomycin, and αCD95, or STS. After 180 min, the percentage of apoptotic and necrotic cells was counted, and DNA-fragmentation was quantitated by use of the BM Cell Death Detection ELISA.

Results

Jurkat cells maintained in a glucose-free RPMI 1640 medium, supplemented with 2 mM pyruvate and challenged with STS or αCD95 showed apoptotic changes within 2-3 h. Exposure to either stimulus induced apoptosis with similar frequency and kinetics. For reasons of clarity, mainly data for STS are shown Figure 1. For ATP-depletion we used oligomycin, which reduced the intracellular concentration of ATP within 45 min to ≤10 % (as compared to untreated control cells). Stimulated cells, depleted of ATP, died with necrotic features Figure 1. Oligomycin itself was not toxic during the period of the experiment and could be replaced e.g., by CCCP, a mitochondrial uncoupler. When glucose was added to STS- plus oligomycin-treated cells, ATP was generated by glycolysis and the mode of cell death changed from apoptotic to necrotic Figure 1B. These data show that the shape of cell death, apoptosis or necrosis, in this system does not depend on the type of stimuli used for challenge, but is dependent on intracellular ATP levels. Further confirmation was derived from experiments where ATP was only partially depleted: ATP-concentrations of 50-100% allowed the execution of cell death by apoptosis. In cell populations with ATP levels of 30-50%, death occurred by apoptosis and necrosis. When ATP concentrations dropped below 30%, cells died exclusively by necrosis.

For further characterization of the ATP-dependence of individual apoptotic processes, DNA fragmentation, intracellular proteolysis, and phosphatidylserine translocation were quantitated in the different models of cell death. Oligonucleosomal DNA fragmentation was activated exclusively in apoptotic cell death and was not detectable in necrotic cells even after rupture of the cell membrane Figure 2. Similar data were obtained for DNA-cleavage into 300/50 kbp fragments. Also lamins, important structures for the architecture of the nucleus, were proteolytically degraded during apoptosis only. Translocation of PS to the outer leaflet of the plasma membrane (staining by anne-

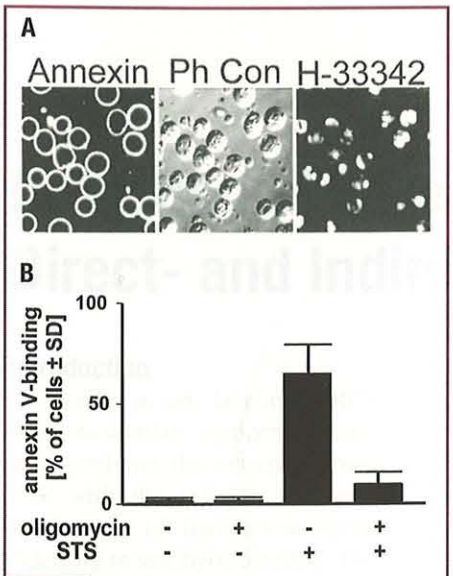

Figure 3 **Phosphatidylserine translocation in apoptotic, but not in necrotic cells.**
(A) Jurkat cells were incubated with STS and after 120 min, stained with H-33342 (for chromatin) and FITC-annexin V (for PS). Confocal microscope images of the same group of cells show apoptotic chromatin condensation (right, blue fluorescence) and strong staining of the plasma membrane due to staining with annexin V (left, green fluorescence). At the time of recording, all cells had a plasma membrane that was impermeable to propidium iodide. **(B)** Jurkat cells were incubated with STS + oligomycin as indicated. After 90 min cells were stained with annexin-FITC, and the number of positive cells was quantitated.

xin V, see Figure 3) occurred in apoptotic cells within one hour. ATP-depletion or induction of necrosis, respectively, prevented PS translocation. This suggests that stainability with annexin V is a specific marker for apoptosis. Use of confocal microscopy instead of FACS analysis even allows the selective identification of apoptosis by annexin staining in adherent cell populations e.g., neurons [6].

In the model described here, the execution of apoptosis or necrosis can be induced under controlled conditions by the same stimulus in a single cell line. Therefore, this model is suitable for testing methods that may be used to distinguish between, and to quantitate, the two modes of cell death. In Figure 2B a comparison of the data from the BM Cell Death Detetection ELISA and data based on counting cells according to morphological criteria, is shown for different cell death models. The excellent correlation between morphologically defined apoptosis and ELISA data not only applies to different models of apoptotic cell death, but also holds true when apoptosis was modulated e. g., by zVADfmk (an inhihibitor of caspases, a family of thiolproteases necessary for cell death triggered by CD95). In contrast to more time consuming morphologic and electrophoretic methods, the BM Cell Death Detection ELISA allows the simultaneous analysis of many samples. Due to the high sensitivity, a cell number of 200-1000 cells is sufficient for the quantitation of DNA fragmentation by ELISA.

Discussion

In the experimental model described here, the BM Cell Death Detection ELISA and staining with annexin V showed good correspondence with other apoptotic endpoints, and proved to be selective for the detection of apoptosis (also in the presence of necrosis) Figure 4. Despite the good correlation in the experimental models described here, it seems to be necessary to verify the selective detection/quantitation of apoptosis in each new model by an initial comparison with other methods. Once such a correlation has been established, the BM Cell Death Detection ELISA provides an efficient tool for the selective quantitation of apoptotic cells in extensive experiments with large numbers of samples. For example, we found a good correlation between data obtained with the ELISA method and the apoptosis rate (quantitated by morphological methods) in hepatocyte cultures [5]. Another example with similarly good correlations is the induction of cell death in macrophages exposed to intracellular pathogens or toxins. In these experiments, apoptotic cell death (and not necrosis) was selectively detected with the BM Cell Death Detection ELISA and by annexin V staining [7]. Moreover, the specificity of the BM Cell Death Detection ELISA for the detection of apoptosis even applies to a certain extent, to pathologic processes *in vivo*. Liver failure, induced by TNF or activation of CD95 (Fas/Apo-1), is associated with an initial increase of the apoptosis rate and DNA-fragmentation, detectable by the BM Cell Death Detection ELISA [5]. A subsequent dramatic increase in the percentage of necrotic cells did not cause a respective rise in the values obtained with the BM Cell Death Detection ELISA. Thus, the detection of apoptosis by the ELISA method was detected relatively selectively even in the presence of an excess of necrotic cells [8, 9]. One of the potential drawbacks of the ELISA method for certain applications is that apoptosis is analyzed in a population of cells and can therefore not be correlated with other

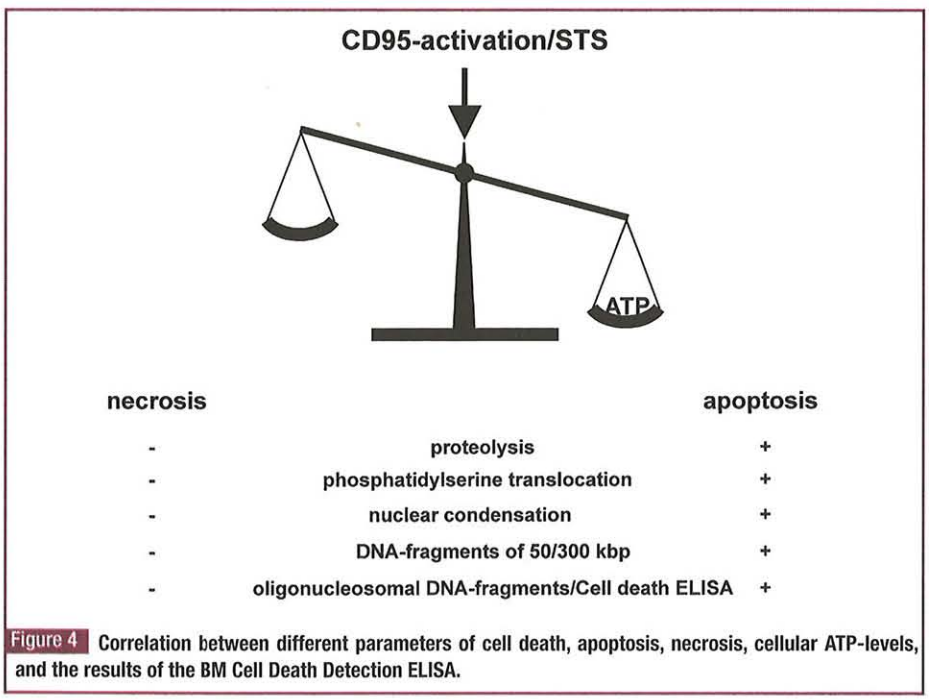

Figure 4 **Correlation between different parameters of cell death, apoptosis, necrosis, cellular ATP-levels, and the results of the BM Cell Death Detection ELISA.**

processes at the level of the individual cell. In this case, staining with annexin V may provide a useful alternative. Annexin V-staining showed a similar specificity for apoptotic cells as the ELISA method. The ELISA can be applied to cell populations Figure 3 as well as annexin V to individual cells in combination with other methods [6].

Product	Cat.No.	Pack Size
Cell Death Detection ELISA	1 544 675	96 tests
ATP Bioluminescence Assay Kit CLS II	1 699 695	1600 assays (MTP), 800 assays (tube)
ATP Bioluminescence Assay Kit HS II	1 699 709	1000 assays (MTP), 500 assays (tube)
Annexin-V-FLUOS	1 828 681	250 tests

References

1. Kerr, J.F., Wyllie, A.H., and Currie, A.R. (1972) Apoptosis: A basic biological phenomenon with wide-ranging implications in tissue kinetics. *Br. J. Cancer* **26**: 239-247.
2. Leist, M., Nicotera, P. (1997) The shape of cell death. *Biochem. Biophys. Res. Commun.* **236**: 1-9.
3. Nicotera, P., Leist, M. (1997) Energy supply and the shape of death in neurons and lymphoid cells. *Cell Death Differ.* **4**: 435-442.
4. Leist, M., Single, B., Castoldi, A.F., Kühnle, S., and Nicotera P (1997) Intracellular ATP concentration: a switch deciding between apoptosis and necrosis. *J. Exp. Med.* **185**: 1481-1486.
5. Leist, M., Gantner, F., Bohlinger, I., Tiegs, G., Wendel, A. (1994) Use of the cell death detection ELISA to detect TNF-induced DNA-fragmentation. *Biochemica* **3**: 18-20.
6. Leist, M., Volbracht, C., Kühnle, S., Fava, E., Ferrando-May, E., and Nicotera, P. (1997) Caspase-mediated apoptosis in neuronal excitotoxicity triggered by nitric oxide. *Mol. Med.* **3**: 750-764.
7. Barsig, J., Kaufmann, S.H. (1997) The mechanism of cell death in *Listeria monocytogenes*-infected murine macrophages is distinct from apoptosis. *Infect. Immun.* **65**: 4075-4081.
8. Leist, M., Gantner, F., Künstle, G., Bohlinger, I., Tiegs, G., Bluethmann, H., and Wendel, A. (1996) The 55 kD tumor necrosis factor receptor and CD95 independently signal murine hepatocyte apoptosis and subsequent liver failure. *Mol. Med.* **2**: 109-124.
9. Leist, M., Gantner, F., Bohlinger, I., Tiegs, G., Germann, P.G., and Wendel, A. (1995) Tumor necrosis factor-induced hepatocyte apoptosis precedes liver failure in experimental murine shock models. *Am. J. Pathol.* **146**: 1220-1234.